A COMPARISON OF SPECIFIC HEAT RATIO MODELS FOR CYLINDER PRESSURE MODELING

Marcus Klein and Lars Eriksson

Vehicular Systems, Dept of EE
Linköpings Universitet
SWEDEN
Email: klein@isy.liu.se

Abstract: An accurate specific heat ratio model is important for an accurate heat release analysis, since the specific heat ratio couples the systems energy to other thermodynamic quantities. The objective is therefore to investigate models of the specific heat ratio for the single-zone heat release model, and find a model accurate enough to introduce a cylinder pressure modeling error less than or in the order of the cylinder pressure measurement noise, while keeping the computational complexity at a minimum. Based on assumptions of frozen mixture for the unburned mixture and chemical equilibrium for the burned mixture, the specific heat ratio is calculated using a full equilibrium program for an unburned and a burned air-fuel mixture, and compared to already existing and newly proposed models of γ.

A two-zone mean temperature model and the Vibe function are used to parameterize the mass fraction burned. The mass fraction burned is used to interpolate the specific heats for the unburned and burned mixture, and then form the specific heat ratio, which renders a small enough modeling error in γ. The impact that this modeling error has on the cylinder pressure is less than that of the measurement noise. The specific heats for the unburned mixture are captured within 0.2 % by linear functions, and the specific heats for the burned mixture are captured within 1 % by higher-order polynomials for the major operating range of a spark ignited (SI) engine.

1. INTRODUCTION

The accuracy with which the energy balance can be calculated for a combustion chamber depends in part on how accurately changes in the internal energy of the cylinder charge are represented. The most important thermodynamic property used when calculating the heat release rates in engines is the ratio of specific heats, $\gamma(T, p, \lambda) = \frac{c_p}{c_v}$ (Gatowski et al., 1984; Chun and Heywood, 1987; Guezennec and Hamama, 1999).

Based on the first law of thermodynamics, Gatowski et al. (1984) developed a single-zone heat release model that has been widely used, where the specific heat ratio is represented by a linear function in mean charge temperature T:

$$\gamma_{lin}(T) = \gamma_{300} + b(T - 300) \qquad (1)$$

This allows a critical examination of the burning process by analysis of the heat release. In order to compute the heat release correctly, the parameters in the single-zone model need to be well tuned. These parameters, such as heat transfer coefficients, γ_{300} and b in the linear γ-model (1) and so on, can be tuned using well known methods. For instance, Eriksson (1998) uses standard prediction error methods to tune the parameters. This is done by minimizing the prediction error of the measured cylinder pressure, i.e. by minimizing the difference between the modeled and measured cylinder pressure. Applying these standard methods usually ends up in absurd and non-physical values of γ_{300}, as it becomes larger than 1.40, which is the value of γ_{300} for pure air. But more importantly, the linear approximation of γ (1) itself introduces a model error in the cylinder pressure which has a root mean square error of approximately 30 kPa, for low load engine operating points, and approximately 90 kPa in the mean for operating points covering the entire operating range. These errors are more

than four and ten times the error introduced by the measurement noise, and will affect the computed heat release. Therefore a better model of $\gamma(T, p, \lambda)$ is sought. A correct model of $\gamma(T, p, \lambda)$ is also desirable in order to avoid badly tuned (biased) parameters.

The objective is to investigate models of the specific heat ratio for the single-zone heat release model, and find a model accurate enough to introduce a modeling error less than or in the order of the cylinder pressure measurement noise, while keeping the computational complexity at a minimum. Such a model would help us to compute a more accurate heat release trace.

1.1 Outline

In the following section three existing γ-models are described. Then based on chemical equilibrium, a reference model for the specific heat ratio is described. Thereafter, the reference model is calculated for an unburned and a burned air-fuel mixture respectively, and compared to these existing models in the two following sections. With the knowledge of how to describe γ for the unburned and burned mixture respectively, the focus is turned to finding a γ-model during the combustion process, i.e. for a partially burned mixture. This is done in section 6, where a number of approximative models are proposed. These models are evaluated in terms of the normalized root mean square error related to the reference γ-model found from chemical equilibrium, as well as the influence the models have on the cylinder pressure, and also in terms of computational time.

2. EXISTING MODELS OF γ

The computational time involved in repeated use of a full equilibrium program, such as CHEPP (Eriksson, 2004) or the NASA program (Svehla and McBride, 1973), can be substantial, and therefore models of the thermodynamic properties have been developed. Three such models will now be described.

2.1 Linear model in T

The specific heat ratio during the closed part of the cycle, i.e. when both intake and exhaust valves are closed, is most frequently modeled as either a constant, or as a linear function of temperature. The latter model is used in (Gatowski et al., 1984), where it is stated that the model approximation is in parity with the other approximations made for this family of single-zone heat-release models. The linear function in T can be written as:

$$\gamma_{lin}(T) = \gamma_{300} + b\,(T - 300) \qquad (2)$$

Depending on which temperature region and what air-fuel ratio λ the model will be used for, the slope

b and constant γ_{300} in (2) have to be adjusted. Concerning the temperature region, this shortcoming can be avoided by increasing the complexity of the model and use a second (or higher) order polynomial for $\gamma_{lin}(T)$. This has been done in for example Brunt et al. (1998). Such an extension reduces the need for having different values of γ_{300} and b for different temperature regions. Later on, $\gamma_{lin}(T)$ is calculated in a least squares sense for both burned and unburned mixtures.

2.2 Segmented linear model in T

According to Chun and Heywood (1987), the commonly made assumption that $\gamma(T)$ is constant or a linear function of mean temperature is not sufficiently accurate. Instead, they propose a segmentation of the closed part of the engine cycle into three segments; compression, combustion and post-combustion (expansion). Both the compression and post-combustion are modeled by linear functions of T, while the combustion event is modeled by a constant γ. They further state that with these assumptions, the one-zone analysis framework will provide accurate enough predictions. The model of γ can be written as:

$$\gamma_{seg}(T, x_b) = \begin{cases} \gamma_{300}^{comp} + b^{comp}\,(T - 300) & x_b < 0.01 \\ \gamma_{300}^{comb} & 0.01 \leq x_b \leq 0.99 \\ \gamma_{300}^{exp} + b^{exp}\,(T - 300) & x_b > 0.99 \end{cases}$$
$$(3)$$

where the mass fraction burned x_b is used to classify the three phases. The γ-model proposed by Chun and Heywood (1987) has discontinuities when switching between the phases compression, combustion and post-combustion. This can pose a problem when estimating e.g. the mass fraction burned.

2.3 Polynomial model in p and T

The third model is a polynomial model of the internal energy u developed in Krieger and Borman (1967) for combustion products of C_nH_{2n}, e.g. iso-octane. For weak and stoichiometric mixtures ($\lambda \geq 1$), a single set of equations could be stated, whereas different sets where found for each $\lambda < 1$. The model of u for $\lambda \geq 1$ is given by:

$$u(T, p, \lambda) = A(T) - \frac{B(T)}{\lambda} + u_{corr}(T, p, \lambda) \qquad (4)$$

given in [kJ/(kg of original air)], where

$$A(T) = a_1 T + a_2 T^2 + \ldots + a_5 T^5 \qquad (5a)$$

$$B(T) = b_0 + b_1 T + \ldots + b_4 T^4 \qquad (5b)$$

The gas constant was found to be:

$$R(T, p, \lambda) = 0.287 + \frac{0.020}{\lambda} + R_{corr}(T, p, \lambda) \qquad (6)$$

given in [kJ/(kg of original air) K]. Krieger and Borman suggested that the correction terms u_{corr} and R_{corr} should account for dissociation, and that they are non-zero for $T > 1450$ K. They

correction terms as well as the coefficient values for the polynomials in (5)-(6) are given in (Klein and Eriksson, 2004).

In general, the error in u was found to be less than 2.5 per cent in the pressure and temperature range of interest, where the extreme end states were approximately $\{2300\ K,\ 0.07\ MPa\}$ and $\{3300\ K,\ 35\ MPa\}$, and less than 1 per cent over most of the range. A model of γ is then found as

$$\gamma_{KB} = \frac{c_p}{c_v} = 1 + \frac{R}{c_v} \qquad (7)$$

where R is given by (6) and $c_v = \frac{\partial u}{\partial T}$ is found by differentiating (4) with respect to T.
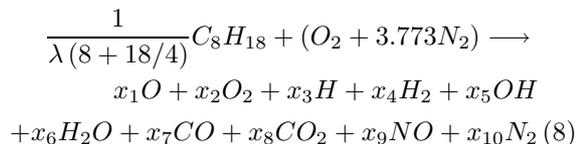
2.4 *Summary of existing γ-models*

Apparently there are ambiguities in which model structure to use for γ, therefore $\gamma(T, p, \lambda)$ is calculated for adequate temperature and pressure regions for both unburned and burned mixture, assuming that the unburned cylinder charge is frozen and the burned mixture is at equilibrium at every instant. This in order to find out what model structure of γ that is accurate enough for our purposes. One such purpose is to estimate parameters in the single-zone model such as heat transfer coefficients, burn rate parameters and so on, using the measured cylinder pressure. This requires a model of the cylinder pressure in which the γ-model has a key role, and therefore the impact each γ-model has on the cylinder pressure is monitored. All thermodynamic properties depend on the air-fuel ratio λ, but for notational convenience this dependence is hereafter left out when there is no explicit dependence.

3. CHEMICAL EQUILIBRIUM

Assuming that the unburned air-fuel mixture is frozen and that the burned mixture is at equilibrium at every instant, the specific heat ratio and other thermodynamic properties of various species can be calculated using the Matlab package CHEPP. The results from CHEPP have been validated to give accurate results with the given assumptions (Eriksson, 2004). Therefore if the assumptions of unburned frozen mixture and burned mixture at chemical equilibrium are valid, CHEPP captures the behavior of the actual experimental mixture in the cylinder fully. According to Heywood (1988, p.86), it is a good approximation for performance estimates to consider the unburned gases as frozen and the burned gases as in chemical equilibrium during the closed part of the engine cycle. As a consequence, CHEPP is believed to capture the thermodynamic properties of a air-fuel mixture well.

The fuel considered is a reference fuel named iso-octane, C_8H_{18}, which reacts with air according to:

$$\frac{1}{\lambda(8 + 18/4)}C_8H_{18} + (O_2 + 3.773N_2) \longrightarrow$$
$$x_1O + x_2O_2 + x_3H + x_4H_2 + x_5OH$$
$$+x_6H_2O + x_7CO + x_8CO_2 + x_9NO + x_{10}N_2 \ (8)$$

where the products given on the right hand side are chosen by the user and λ is the air-fuel ratio (AFR). The coefficients x_i are found by CHEPP and when scaled properly with λ they reveal the mole fraction of specie i that the mixture consists of at a given temperature, pressure and air-fuel ratio. The mixture is assumed to obey the Gibbs-Dalton law.

4. UNBURNED MIXTURE

First of all, the specific heat ratio for an unburned frozen mixture of iso-octane is computed using CHEPP in the temperature region $T \in [300, 1000]$ K, which is valid for the entire closed part of a motored cycle. The specific heat ratio for air-fuel ratio $\lambda = 1$ is shown in figure 1 as a function of temperature, together with its linear approximation (2) in a least squares sense. The linear approximation γ_{lin}^u is fairly good for $\lambda = 1$. Actually, the specific heats c_p and c_v from which γ is formed, are fairly well described by linear functions of temperature. Table 1 summarizes the normalized RMSE (NRMSE) and the coefficients of the respective linear function for γ, mass-specific heats c_v and c_p for temperature region $T \in [300, 1000]$ K and $\lambda = 1$. The RMSE of γ_{lin}^u is defined as:
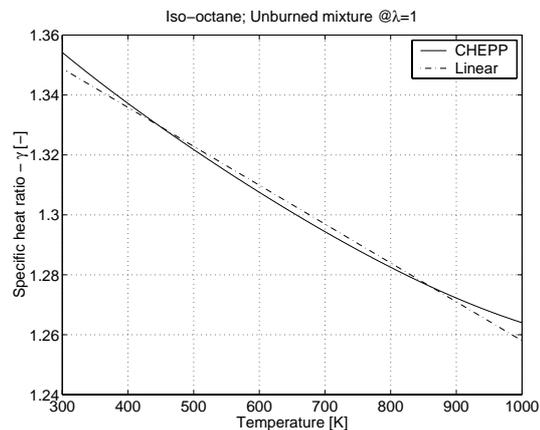

Fig. 1. Specific heat ratio for unburned stoichiometric mixture using CHEPP and the corresponding linear function of temperature.

Property	Constant	Slope	NRMSE
γ_{lin}^u [-]	1.3488	$-13.0 \cdot 10^{-5}$	0.19 %
$c_{p,u}^{lin}$ [J/(kg K)]	1051.9	0.387	0.15 %
$c_{v,u}^{lin}$ [J/(kg K)]	777.0	0.387	0.20 %

Table 1. Coefficients and normalized RMSE in linear approximations of γ, mass-specific c_v and c_p, for temperature region $T \in [300, 1000]$ K and $\lambda = 1$
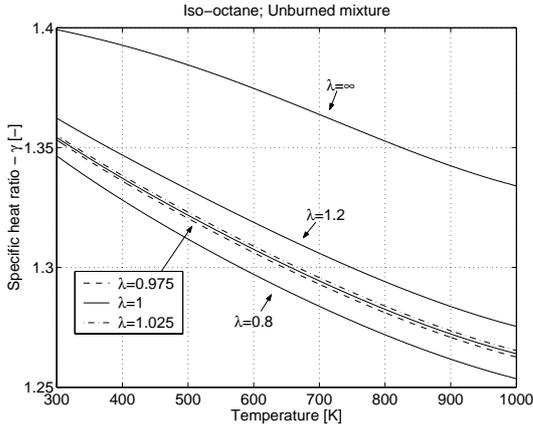
Fig. 2. Specific heat ratio for unburned stoichiometric mixture using CHEPP for various air fuel ratios λ as functions of temperature. $\lambda = \infty$ corresponds to pure air.

$$RMSE = \sqrt{\frac{1}{M} \sum_{j=1}^{M} (\gamma(T_j) - \gamma_{lin}^u(T_j))^2} \quad (9)$$

where M are the number of samples. The NRMSE is then found by normalizing RMSE with the mean value of $\gamma(T)$:

$$NRMSE = \frac{RMSE}{\frac{1}{M} \sum_{j=1}^{M} \gamma(T_j)} \quad (10)$$

Besides temperature, the specific heat ratio also varies with AFR, as shown in figure 2 where λ is varied between 0.8 (rich) and 1.2 (lean). For comparison, $\gamma(T)$ is also shown for $\lambda = \infty$, i.e. pure air which corresponds to fuel cut-off.

The coefficients in γ_{lin}^u (2) vary with λ as shown in the two upper plots of figure 3. Both the constant γ_{300} and the slope b become smaller as the air-fuel ratio becomes richer. From the bottom plot of figure 3, which shows the NRMSE for different AFR:s, it can be concluded that the linear approximation $\gamma_{lin}^u(T)$ is better the leaner the mixture is, at least for $\lambda \in [0.8, 1.2]$.

5. BURNED MIXTURE

The specific heat ratio γ for a burned mixture of iso-octane is computed using CHEPP in temperature region $T \in [500, 3500]$ K and pressure region $p \in [0.25, 100]$ bar, which covers most of the closed part of a firing cycle. The mixture is assumed to be at equilibrium at every instant. The specific heat ratio is strongly dependent on mixture temperature T, but γ also depends upon the air-fuel ratio λ and pressure p as shown in figure 4 and figure 5 respectively. For the same deviation from $\lambda = 1$, rich mixtures tend to deviate more from the stoichiometric mixture, than lean mixtures do. The pressure dependence of γ is only visible for $T > 1500$ K, and a higher pressure tends to retard the dissociation and yields a higher γ.
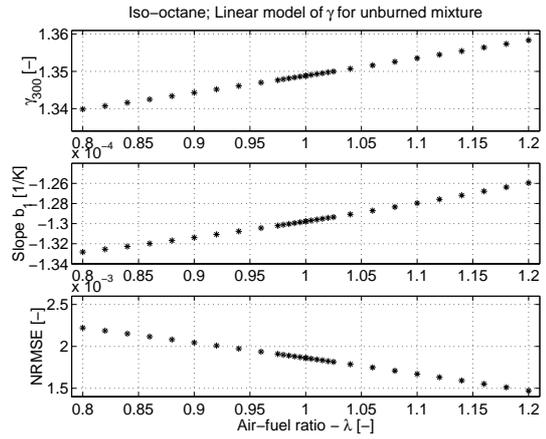

Fig. 3. *Upper:* The constant value γ_{300} in (2) as a function of λ for unburned mixture at equilibrium. *Middle:* The value of the slope coefficient b in (2) as a function of AFR. *Bottom:* Normalized root mean square error (NRMSE) for $\gamma_{lin}^u(T)$.
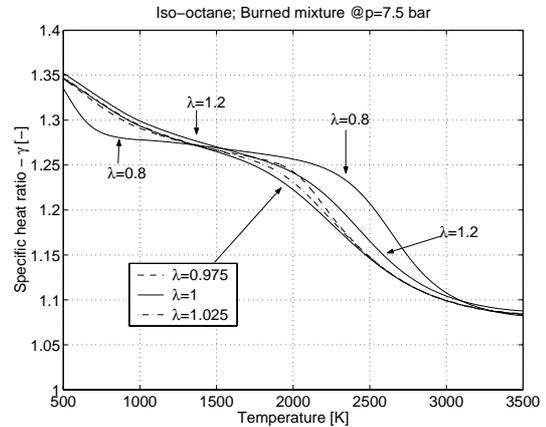

Fig. 4. Specific heat ratio for burned mixture at various air-fuel ratios λ at 7.5 bar using CHEPP.

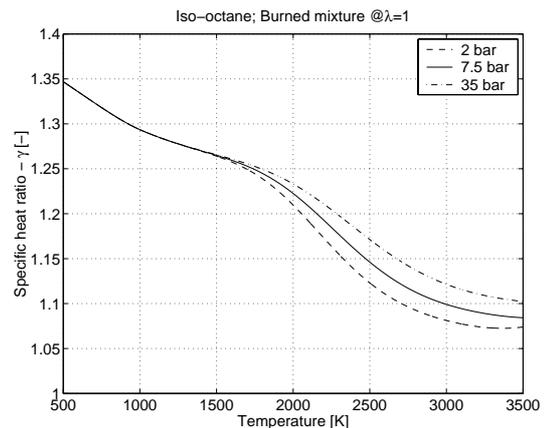Fig. 5. Specific heat ratio for burned stoichiometric mixture using CHEPP at various pressures.

To model the specific heat ratio with a linear function $\gamma_{lin}^b(T)$ of temperature, and thereby neglecting the dependence of pressure, will of course introduce a modeling error. This modeling error depends on which temperature (and pressure) region the linear function is estimated for, since different regions will
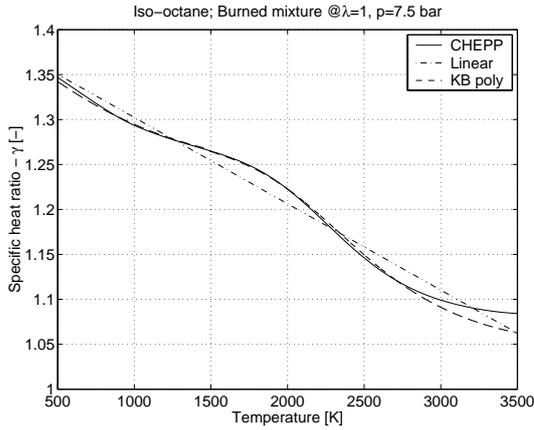
Fig. 6. Specific heat ratio for burned stoichiometric mixture using CHEPP, the corresponding linear function γ_{lin}^b and Krieger-Bormans polynomial γ_{KB}.

Region	$T \in$	γ_{300}	b
A	[500, 3500]	1.3695	$-9.6 \cdot 10^{-5}$
B	[500, 3000]	1.3726	$-9.9 \cdot 10^{-5}$
C	[500, 2700]	1.3678	$-9.4 \cdot 10^{-5}$
D	[500, 2500]	1.3623	$-8.8 \cdot 10^{-5}$
E	[1200, 3000]	1.4045	$-11.4 \cdot 10^{-5}$

Table 2. Coefficients in linear approximation $\gamma_{lin}^b(T)$ found in (2) for $\lambda = 1$ and $p = 7.5$ bar.

Region	$T \in$	γ_{lin}^b		γ_{KB}	
		MRE	NRMSE	MRE	NRMSE
A	[500, 3500]	2.0 %	0.97 %	2.0 %	0.56 %
B	[500, 3000]	1.6 %	0.95 %	0.7 %	0.20 %
C	[500, 2700]	1.9 %	0.90 %	0.3 %	0.17 %
D	[500, 2500]	2.4 %	0.74 %	0.3 %	0.17 %
E	[1200, 3000]	1.6 %	0.74 %	0.7 %	0.21 %

Table 3. Maximum relative error (MRE) and normalized root mean square error (NRMSE) for different temperature regions at $\lambda = 1$ and $p = 7.5$ bar.

Reg	$\gamma_{KB}@\lambda = 0.975$		$\gamma_{KB}@\lambda = 1$		$\gamma_{KB}@\lambda = 1.025$	
	MRE	NRMSE	MRE	NRMSE	MRE	NRMSE
A	1.9 %	0.86 %	2.0 %	0.56 %	2.1 %	0.59 %
B	1.8 %	0.73 %	0.7 %	0.20 %	0.7 %	0.28 %

Table 4. Maximum relative error (MRE) and normalized root mean square error (NRMSE) for different temperature regions for $\gamma_{KB}(T, p, \lambda)$ at $p = 7.5$ bar and $\lambda = \{0.975, \ 1, \ 1.025\}$

yield different coefficient values in (2). In figure 6 γ is computed at $\lambda = 1$ and $p = 7.5$bar for $T \in [500, 3500]$ K, and as well as the corresponding linear function γ_{lin}^b (2) and the polynomial γ_{KB} (7) developed by Krieger and Borman (1967).

The linear approximation $\gamma_{lin}^b(T)$ does not capture the behavior of $\gamma(T)$ for $\lambda = 1$ very well. The coefficients for the linear model $\gamma_{lin}^b(T)$ vary for the specific temperature region. They are given for temperature regions A to E in Table 2. A second order polynomial shows the same behavior as the linear case, but when the order of the polynomial is increased to three, the model captures the modes of $\gamma(T)$ quite well. By increasing the complexity of the model even more, an even better fit is found. This has been done in the Krieger-Borman polynomial, and for this example it captures the the behavior of $\gamma(T)$ well for temperatures below 2800 K as seen in figure 6 and in the right-most (NRMSE) column in table 3, where the NRMSE value is much higher for temperature region A than for the other regions. In table 3, the NRMSE and maximum relative error (MRE) for the linear approximation γ_{lin}^b and the Krieger-Borman polynomial γ_{KB} at various temperature regions are given. As expected, the Krieger-Borman polynomial is better than the linear approximation in every chosen temperature region, since the NRMSE is smaller. Comparing just the MRE:s could result in false conclusions. Take the temperature region A for instance, where the respective MRE are approximately the same. One could then conclude that the models describe γ equally well, but in figure 6 it was clearly visible that γ_{KB} is the better one, which is also the conclusion when comparing the respective NRMSE.

In table 4, the NRMSE and MRE for the Krieger-Borman polynomial $\gamma_{KB}(T, p, \lambda)$ for λ close to stoichiometric is displayed. For $\lambda \geq 1$ (lean), γ_{KB} fits the equilibrium γ better than for $\lambda < 1$, a tendency which is most evident when comparing the NRMSE for temperature region B. For temperature region A the difference for different λ is less striking,

since the γ_{KB} does not fit γ as well for $T > 3000$ K. Therefore the Krieger-Borman polynomial is preferably only to be used on the lean side. On the rich side and close to stoichiometric (within 2.5 %), the Krieger-Borman polynomial does not introduce an error larger than the linear approximation given in table 3, and γ_{KB} should therefore be used in this operating range.

If a linear model of γ is preferred for computational reasons, the performance of the linear model could be enhanced by proper selection of temperature region. However, the MRE does not decrease for every reduction in interval, as seen when comparing MRE:s for regions D and B in table 3. Thus, the temperature region should be chosen with care by using the NRMSE as measure:

- When using the single-zone temperature T to describe the specific heat ratio of the burned mixture, temperature region B is preferable, since during the closed part $T \leq 3000$ K.
- When using the burned-zone temperature T_b in a two-zone model, temperature region E is recommended, since for most cases $T_b \in [1200, 3000]$. The temperature limits are found by evaluating a number of experimental cylinder pressure traces using (A.1) and (A.7). By chosing region E instead of region B, the NRMSE is reduced by 25%.

6. PARTIALLY BURNED MIXTURE

The specific heat ratio γ as a function of mixture temperature T and air-fuel ratio λ for unburned and burned mixture of air and iso-octane has been investigated in the two previous sections. During the closed part of a motored engine cycle, the previous investigations would be enough since the models of the unburned mixture will be valid for the entire region. When considering firing cycles on the other hand, an assumption of either a purely unburned or a purely burned mixture approach is not valid for the entire combustion chamber during the closed part of the engine cycle.

To describe the specific heat ratio in the single-zone model for a partially burned mixture, the mass fraction burned trace x_b is used to interpolate the (mass-)specific heats of the unburned and burned zones to find the single-zone specific heats. The specific heat ratio is then found as the ratio between the interpolated specific heats.

6.1 *Reference model*

The single-zone specific heats are found from energy balance between the single-zone and the two-zone model, from which the single-zone specific heat ratio γ_{CE} can be stated:

$$c_p(T,p,x_b) = x_b\,c_{p,b}(T_b,p) + (1-x_b)\,c_{p,u}(T_u) \quad (11a)$$

$$c_v(T,p,x_b) = x_b\,c_{v,b}(T_b,p) + (1-x_b)\,c_{v,u}(T_u) \quad (11b)$$

$$\gamma_{CE}(T,p,x_b) = \frac{c_p(T,p,x_b)}{c_v(T,p,x_b)} \quad (11c)$$

where the mass fraction burned x_b is used as an interpolation variable. The single-zone (T), burned zone (T_b) and unburned zone (T_u) temperatures are given by the two temperatures models (A.1) and (A.7) described in appendix A. The first is the ordinary single-zone temperature model and the second is a two-zone mean temperature model developed by Andersson (2002). The mass specific heats in (11) are computed using CHEPP (Eriksson, 2004) and γ_{CE} then forms the reference model.

To compute γ_{CE} is computationally heavy. Even when the specific heats are computed before-hand at a number of operating points, the computational burden is still heavy due to the numerous table look-ups and interpolations required. Therefore, a computationally more efficient model which retains accuracy is sought for. A number of γ-models will therefore be described in the following subsection, where they are divided into three subgroups based upon their modeling assumptions. These γ-models are then compared to the reference model γ_{CE} found from (11), in terms of four evaluation criteria, specified in the subsection "Evaluation criteria".

6.1.1. *How to find x_b?*
To compute the specific heat ratio γ_{CE} (11), a mass fraction burned trace x_b is needed. For simulated pressure data, the mass

fraction burned is considered to be known, which is the case in this work. However, if one were to use experimental data to e.g. do heat release analysis, x_b can not be considered to known. There are then two ways of determining the mass fraction burned; The first is to use a simple and computationally efficient method to get x_b from a given cylinder pressure trace. Such methods include the pressure ratio management by Matekunas (1983) described in section E. If one does not settle for this, the second approach is to initialize x_b using a simple method from the first approach, and then iteratively refine the mass fraction burned trace x_b using the computed heat release.

6.2 *Grouping of γ-models*

Twelve γ-models have been investigated and based upon their modeling assumptions, they are divided into three subgroups; The first group contains models for *burned mixture* only. The second contains models based on *interpolation of the specific heat ratios* directly, and the third group, to which (11) belongs, contains the models based on *interpolation of the specific heats*, from which the ratio is determined.

6.2.1. *Group $\mathcal{B}$: Burned mixture*
The first subgroup represents the in-cylinder mixture as a single zone of burned mixture with single-zone temperature T, computed by (A.1). The first model, denoted $\mathcal{B}_1$, is the linear approximation in (2):

$$\gamma_{\mathcal{B}_1}(T) = \gamma_{lin}^b(T) = \gamma_{300} + b\,(T-300) \quad (12)$$

where the coefficients can be determined in at least two ways; One way is to use the coefficients that are optimized for temperature region $T \in [500, 3000]$ (region B in Table 2) for a burned mixture. This approach is used in (Gatowski et al., 1984), although the coefficients differ somewhat compared to the ones given in Table 2. Another way is to optimize the coefficients from the reference model (11). This approach will be the one used here, since it yields the smallest modeling errors in both γ and cylinder pressure p. The approach has optimal conditions for the simulations, and will therefore give the best results possible for this model structure.

The second model, denoted $\mathcal{B}_2$, is the Krieger-Borman polynomial described in (4)

$$u = A(T) - \frac{B(T)}{\lambda} \longrightarrow \gamma_{\mathcal{B}_2}(T) = \gamma_{KB}(T) \quad (13)$$

without the correction term for dissociation. The Krieger-Borman polynomial is used in model $\mathcal{B}_3$ as well,

$$u = A(T) - \frac{B(T)}{\lambda} + u_{corr}(T,p,\lambda)$$
$$\longrightarrow \gamma_{\mathcal{B}_3}(T,p) = \gamma_{KB}(T,p) \quad (14)$$

with the correction term $u_{corr}(T, p, \lambda)$ for dissociation included. The fourth and simplest model uses a constant γ:

$$\gamma_{\mathcal{B}_4} = constant \tag{15}$$

As for model $\mathcal{B}_1$, the coefficient in (15) is determined from the reference model (11).

6.2.2. *Group $\mathcal{C}$: Interpolation of specific heat ratios*

The second subgroup uses a two-zone model, i.e. a burned and an unburned zone, and calculates the specific heat ratio $\gamma_b(T_b)$ and $\gamma_u(T_u)$ for each zone respectively, where the temperatures are given by the two-zone mean temperature model (A.7). The mass fraction burned trace x_b is then used to find the single-zone γ by interpolating γ_b and γ_u. Note that the energy balance equation, used in (11), is not fulfilled for subgroup $\mathcal{C}$.

The first model, denoted $\mathcal{C}_1$, interpolates linear approximations of γ for the unburned and burned mixture. The linear functions are optimized in temperature region $T \in [300, 1000]$ for the unburned mixture, and temperature region $T \in [1200, 3000]$ for the burned mixture. The resulting $\gamma_{\mathcal{C}_1}$ can therefore be written as:

$$\gamma_{\mathcal{C}_1}(T, x_b) = x_b \, \gamma_{lin}^b(T_b) + (1 - x_b) \, \gamma_{lin}^u(T_u) \tag{16}$$

where the coefficients for the linear functions are given in Table 2 and Table 1 respectively.

The second model was proposed in (Stone, 1999, p.423), here denoted $\mathcal{C}_2$, and is based on interpolation of the internal energy u computed from the Krieger-Borman polynomial:

$$u = A(T) - x_b \frac{B(T)}{\lambda} \longrightarrow \gamma_{\mathcal{C}_2}(T, x_b) \tag{17}$$

This model includes neither dissociation nor the internal energy of the unburned mixture.

An improvement of model $\mathcal{C}_1$ is expected when substituting the linear model for the burned mixture with the Krieger-Borman polynomial. This new model is denoted $\mathcal{C}_3$ and described by:

$$\gamma_{\mathcal{C}_3}(T, p, x_b) = x_b \, \gamma_{KB}(T_b, p) + (1 - x_b) \, \gamma_{lin}^u(T_u) \tag{18}$$

The fourth model interpolates $\gamma_u(T_u)$ and $\gamma_b(T_b, p)$ given by CHEPP:

$$\gamma_{\mathcal{C}_4}(T, p, x_b) = x_b \, \gamma_b(T_b, p) + (1 - x_b) \, \gamma_u(T_u) \tag{19}$$

and this model is denoted $\mathcal{C}_4$. This model will reflect the modeling error introduced by interpolating the specific heat ratios directly instead of using the definition through the specific heats (11). The segmented linear model (3) developed by Chun and Heywood (1987) is also investigated and here denoted by model $\mathcal{C}_5$:

$$\gamma_{\mathcal{C}_5}(T, x_b) = \begin{cases} \gamma_{300}^{comp} + b^{comp}(T - 300) & x_b < 0.01 \\ \gamma_{300}^{comb} & 0.01 \le x_b \le 0.99 \\ \gamma_{300}^{exp} + b^{exp}(T - 300) & x_b > 0.99 \end{cases} \tag{20}$$

Model $\mathcal{C}_5$ uses the single-zone temperature for each phase, and classifies into group $\mathcal{C}$ due to that the switching used for x_b in (20) can be seen as a

nearest neighbor interpolation. As for model $\mathcal{B}_1$ and $\mathcal{B}_4$, the coefficients in (20) are determined from the reference model (11).

6.2.3. *Group $\mathcal{D}$: Interpolation of specific heats*

The last subgroup uses a two-zone model, i.e. a burned and an unburned zone, just as the second subgroup, and the specific heats are interpolated to get the single-zone specific heats. The first model, denoted $\mathcal{D}_1$, uses the Krieger-Borman polynomial for the burned zone to find $c_{p,b}(T_b, p)$ and $c_{v,b}(T_b, p)$, and the linear approximations of $c_{p,u}(T_u)$ and $c_{v,u}(T_u)$ given in Table 1 for the unburned zone:

$$\gamma_{\mathcal{D}_1}(T, p, x_b) = \frac{x_b \, c_{p,b}^{KB}(T_b, p) + (1 - x_b) \, c_{p,u}^{lin}(T_u)}{x_b \, c_{v,b}^{KB}(T_b, p) + (1 - x_b) \, c_{v,u}^{lin}(T_u)} \tag{21}$$

An extension of model $\mathcal{D}_1$ is to use the unburned specific heats $c_{p,u}(T_u)$ and $c_{v,u}(T_u)$ computed from CHEPP:

$$\gamma_{\mathcal{D}_2}(T, p, x_b) = \frac{x_b \, c_{p,b}^{KB}(T_b, p) + (1 - x_b) \, c_{p,u}(T_u)}{x_b \, c_{v,b}^{KB}(T_b, p) + (1 - x_b) \, c_{v,u}(T_u)} \tag{22}$$

This model is denoted $\mathcal{D}_2$ and reflects the model error introduced by using the linear approximation of the unburned mixture specific heats, when comparing to $\mathcal{D}_1$.

Model $\mathcal{D}_1$ is also extended for the burned mixture, where the specific heats for the burned mixture $c_{p,b}(T_b, p)$ and $c_{v,b}(T_b, p)$ are computed using CHEPP. This model is denoted $\mathcal{D}_3$:

$$\gamma_{\mathcal{D}_3}(T, p, x_b) = \frac{x_b \, c_{p,b}(T_b, p) + (1 - x_b) \, c_{p,u}^{lin}(T_u)}{x_b \, c_{v,b}(T_b, p) + (1 - x_b) \, c_{v,u}^{lin}(T_u)} \tag{23}$$

and reflects the model error introduced by using the Krieger-Borman approximation of the specific heats, when comparing to $\mathcal{D}_1$.

The reference model γ_{CE} (11) belongs to this group and is denoted $\mathcal{D}_4$:

$$\gamma_{\mathcal{D}_4}(T, p, x_b) = \gamma_{CE}(T, p, x_b) \tag{24}$$

6.3 *Evaluation criteria*

The different γ-models given by (12)-(23) are evaluated in terms of four criteria. The criteria are:

(1) Normalized root mean square error (NRMSE) in γ, which gives a measure of the mean error in γ.

(2) Maximum relative error (MRE) for γ, which yields a measure of the maximum error in γ.

(3) Root mean square error (RMSE) for the corresponding cylinder pressures. This measure will give a measure of the impact that a certain model error has on the cylinder pressure and will help to find a γ-model accurate enough for the single-zone model.

(4) The computational efficiency is also evaluated by comparing the required simulation time of

the cylinder pressure given a burn rate trace and a specific γ-model.

6.4 Evaluation covering one operating point

At first, only one operating point is considered. This operating point is given by the parameter values in table E.1, and corresponds to the cylinder pressure given in figure 7, i.e. at low engine load conditions. The cylinder pressure given in figure 7 is used as an example that illustrates the effect that each model has on specific heat ratio γ and cylinder pressure. To investigate if the engine operating condition influences the choice of model, nine operating points covering most parts of the operating range of an engine are used to do the same evaluations. These operating points and their corresponding cylinder pressures are given in (Klein, 2004, pp.131).
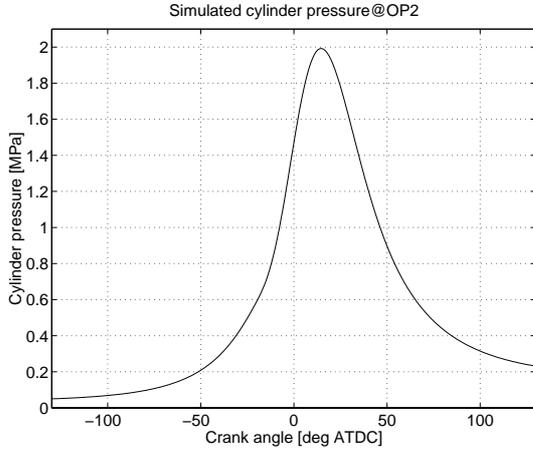
Fig. 7. Simulated cylinder pressure using Gatowski et al.-model with nominal values in table E.1, and the linear γ-model $\mathcal{B}_1$ replaced by reference model $\mathcal{D}_4$.

6.4.1. γ-domain   The γ-models in the three subgroups are compared to the reference model γ_{CE} (11). A summary of the results are given here while a complete picture is given in (Klein, 2004, pp.134). Figure 8 compares the reference model $\mathcal{D}_4$ with the computed values of γ for a few of these models, namely $\mathcal{B}_1$, $\mathcal{B}_3$, $\mathcal{C}_5$, $\mathcal{C}_4$ and $\mathcal{D}_1$.

Of these models, only model $\mathcal{D}_1$ (21) is able to capture the reference model well. This is confirmed by the MRE(γ) and NRMSE(γ) columns in table 5, where only model group $\mathcal{D}$ yields errors lower than 1% for both columns. Model $\mathcal{C}_4$ deviates only during the combustion, which in this case occurs for $\theta \in [-15, 40]$ deg ATDC. This deviation is enough to yield a NRMSE(γ) which is almost 0.6 %, approximately six times that found for $\mathcal{D}_1$.

Of the models previously proposed in literature, the linear model $\mathcal{B}_1$ (12) has the best performance, although it does not capture the reference model very well, as seen in the upper plot of figure 8. Model $\mathcal{B}_3$ (14) is only able to capture the reference
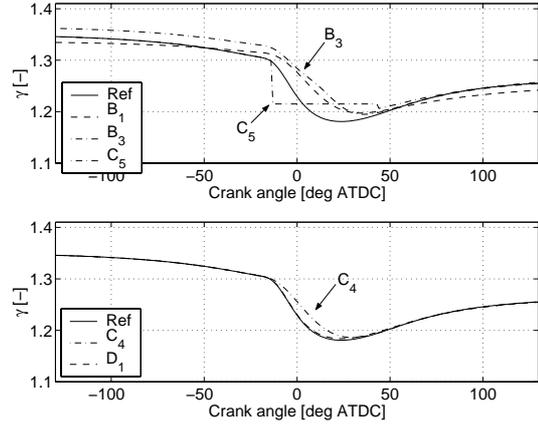
Fig. 8. *Upper:* Specific heat ratios for models $\mathcal{B}_1$, $\mathcal{B}_3$ and $\mathcal{C}_5$ as compared to the reference model $\mathcal{D}_4$. *Lower:* Specific heat ratios for models $\mathcal{C}_4$ and $\mathcal{D}_1$ as compared to the reference model $\mathcal{D}_4$.

Model		MRE: γ [%]	RMSE: p [kPa]	NRMSE: γ [%]	Time [s]
$\mathcal{B}_1$	(12)	4.7	52.3	1.3	3.8
$\mathcal{B}_2$	(13)	5.9	85.8	2.7	4.1
$\mathcal{B}_3$	(14)	5.2	76.0	1.8	4.2
$\mathcal{B}_4$	(15)	7.7	62.8	4.5	3.8
$\mathcal{C}_1$	(16)	2.3	39.8	0.69	4.7
$\mathcal{C}_2$	(17)	7.3	140.7	4.1	4.9
$\mathcal{C}_3$	(18)	2.4	25.4	0.65	5.1
$\mathcal{C}_4$	(19)	2.3	22.8	0.58	211.1
$\mathcal{C}_5$	(20)	8.4	82.9	1.5	4.0
$\mathcal{D}_1$	(21)	0.27	2.8	0.10	5.2
$\mathcal{D}_2$	(22)	0.26	2.6	0.09	12.3
$\mathcal{D}_3$	(23)	0.04	0.3	0.01	381.9
$\mathcal{D}_4$	(11)	0.0	0.0	0.0	384.2

Table 5. Evaluation of γ-models, on the single cycle shown in figure 7.

model after the combustion, since model $\mathcal{B}_3$ is optimized for a burned mixture. Model $\mathcal{C}_5$ (20) has good behavior before and after the combustion. But during the combustion, the constant γ_{300}^{comb} does not capture γ_{CE} very well.

To conclude, model group $\mathcal{D}$ yields errors in γ which are less than 1% for this operating point. Of these models, model $\mathcal{D}_3$ has the best performance compared to the reference model $\mathcal{D}_4$.

6.4.2. *Pressure domain*   The impact that the γ-models have on the corresponding cylinder pressure is shown in figure 9 for models $\mathcal{B}_1$, $\mathcal{B}_3$, $\mathcal{C}_5$, $\mathcal{C}_4$ and $\mathcal{D}_1$, and for all models in (Klein, 2004, pp.138). The plots show the difference between the simulated cylinder pressure for reference model $\mathcal{D}_4$ and the γ-models, i.e. the cylinder pressure error induced by the modeling error in γ. Note that the scaling in the figures are different. The cylinder pressure model used for the simulations is the model developed by Gatowski et al. (1984). Section E gives more details about the implementation used here.

The RMSE of the measurement noise is approximately 6 kPa and it is only model group $\mathcal{D}$ that introduces a modeling error in the same order as the noise in terms of RMSE. Thus, the other γ-
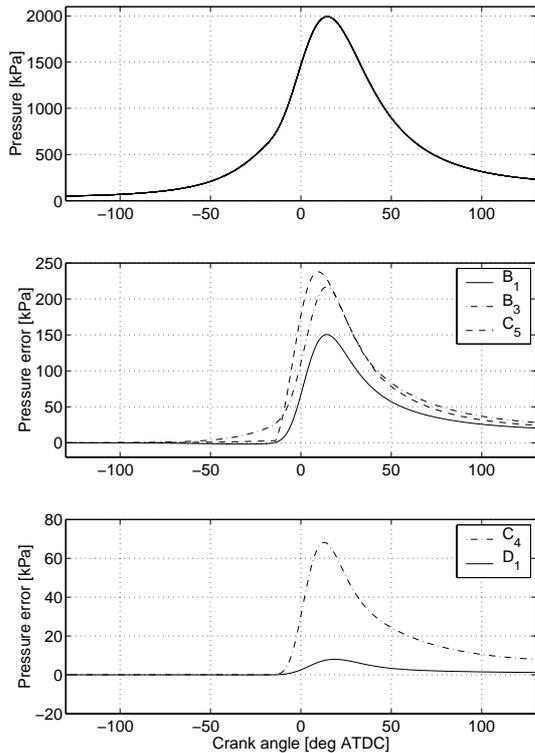
Fig. 9. *Upper:* Reference cylinder pressure, the same as given in figure 7. *Middle:* Cylinder pressure error introduced by models $\mathcal{B}_1$, $\mathcal{B}_3$ and $\mathcal{C}_5$. For convenience, the sign for $\mathcal{C}_5$ is changed. *Lower:* Cylinder pressure error introduced by models $\mathcal{C}_4$ and $\mathcal{D}_1$. Note that the scaling in the plots are different.

models will introduce a modeling error which is significantly larger than the measurement noise as seen in Table 5, and thereby affect the accuracy of the parameter estimates. Within group $\mathcal{D}$, models $\mathcal{D}_3$ and $\mathcal{D}_4$ have the smallest RMSE(p), and therefore yield the highest accuracy. Model $\mathcal{D}_1$ does not introduce a significantly larger RMSE(p) than $\mathcal{D}_2$, and therefore the most time efficient one should be used of these two. Altogether this suggests that any model in group $\mathcal{D}$ could be used.

The previously proposed γ-models $\mathcal{B}_1$, $\mathcal{B}_2$, $\mathcal{B}_3$, $\mathcal{B}_4$ and $\mathcal{C}_5$, described in section 2, all introduce modeling errors which are at least seven times the measurement noise for this operating point. Clearly, a large error, so none of these models are recommended. Of these models, $\mathcal{B}_1$ induces the smallest RMSE(p) and should, if any, be the one used of the previously proposed models.

6.4.3. *A note on crevice volume modeling* Note that the usage of a γ-model different from the linear model used in Gatowski et al. [1984], will also affect the amount of energy left or added to the system when a mass element enters or leaves the crevice volume. This energy term $u' - u = \int_T^{T'}$ has to be restated for every γ-model at hand except model $\mathcal{B}_1$, and this is done for model $\mathcal{D}_1$ in appendix D.

6.4.4. *Computational time* The right-most column of table 5 shows the computational time. The time value given is the mean time for simulating the closed part of one engine cycle using Matlab 6.1 on a SunBlade 100, which has a 64-bit 500 MHz processor. The proposed model $\mathcal{D}_1$ is approximately 70 times faster than the reference model $\mathcal{D}_4$, where the reference model uses look-up tables for precomputed values of the specific heats c_p and c_v. Introducing the model improvement in model $\mathcal{D}_1$ of the specific heat ratio to the Gatowski et al. single-zone heat release model is simple, and it does not increase the computational burden immensely compared to the original setting, i.e. $\mathcal{B}_1$. The increase in computational effort is less than 40 % compared to the linear γ-model when simulating the Gatowski et al. single-zone heat release model.

6.5 *Evaluation covering all operating points*

The same analysis as above has been made for the simulated cylinder pressure from nine different operating points, where $p_{IVC} \in [0.25, 2]$ bar and $T_{IVC} \in [325, 372]$ K. The parameters for each cycle is given in table 6. The operating range in p and T that these cycles cover is given in figure 10, where the upper plot shows the range covered for the unburned mixture, and the lower shows the range covered for single-zone (solid) and burned (dashed) mixture. According to (Heywood, 1988, p.109), the temperature region of interest for an SI engine is 400
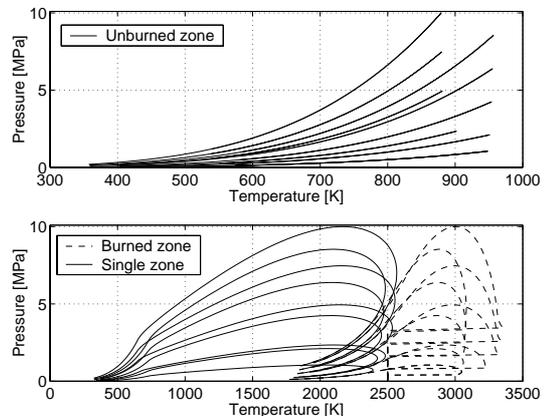

Fig. 10. Operating range in p and T. *Upper:* Unburned zone. *Lower:* Single zone (solid) and burned zone (dashed).

OP	p_{IVC} [kPa]	T_{IVC} [K]	Q_{in} [J]
1	25	372	330
2	50	341	760
3	100	327	1620
4	150	326	2440
5	200	325	3260
1	25	372	330
6	50	372	700
7	100	372	1420
8	150	372	2140
9	200	372	2850

Table 6. Operating points (OP) for the simulated cylinder pressure.

Model	MRE: γ [%]	RMSE: p [kPa]	NRMSE: γ [%]
$\mathcal{B}_1$	3.4	84.9	1.2
$\mathcal{B}_2$	5.2	153.6	2.4
$\mathcal{B}_3$	4.5	137.3	1.7
$\mathcal{B}_4$	7.1	110.0	4.2
$\mathcal{C}_1$	1.9	56.6	0.77
$\mathcal{C}_2$	6.6	269.2	3.9
$\mathcal{C}_3$	1.9	42.4	0.53
$\mathcal{C}_4$	1.8	36.7	0.46
$\mathcal{C}_5$	8.3	191.9	1.6
$\mathcal{D}_1$	0.26	5.8	0.097
$\mathcal{D}_2$	0.25	5.1	0.092
$\mathcal{D}_3$	0.044	0.7	0.016

Table 7. Evaluation of γ-models, in terms of the mean values for all operating points.

to 900 K for the unburned mixture; for the burned mixture, the extreme end states are approximately $\{1200\ K,\ 0.2\ MPa\}$ and $\{2800\ K,\ 3.5\ MPa\}$. Of course, not all points in the range are covered but the cycles at hand cover the extremes of the range of interest.

The results are summarized in terms of MRE, RMSE and NRMSE in table 7 as mean values for all operating point.

6.5.1. *Ordering of models* When comparing the NRMSE for γ in table 7, the ordering of the γ-models, where the best one comes first, is:

$$\mathcal{D}_4 \prec \mathcal{D}_3 \prec \mathcal{D}_2 \prec \mathcal{D}_1 \prec \mathcal{C}_4 \prec \mathcal{C}_3 \prec \mathcal{C}_1 \prec \mathcal{B}_1 \prec$$
$$\mathcal{C}_5 \prec \mathcal{B}_3 \prec \mathcal{B}_2 \prec \mathcal{C}_2 \prec \mathcal{B}_4 \quad (25)$$

Here $\mathcal{B}_2 \prec \mathcal{C}_2$ means that model $\mathcal{B}_2$ is better than $\mathcal{C}_2$. Comparing RMSE for the cylinder pressure p, the ordering of the γ-models becomes:

$$\mathcal{D}_4 \prec \mathcal{D}_3 \prec \mathcal{D}_2 \prec \mathcal{D}_1 \prec \mathcal{C}_4 \prec \mathcal{C}_3 \prec \mathcal{C}_1 \prec \mathcal{B}_1 \prec$$
$$\mathcal{B}_4 \prec \mathcal{B}_3 \prec \mathcal{B}_2 \prec \mathcal{C}_5 \prec \mathcal{C}_2 \quad (26)$$

This ordering is not the same as in (25), but the only difference lies in models $\mathcal{C}_5$ and $\mathcal{B}_4$. Model $\mathcal{C}_5$ has poor performance in terms of RMSE(p), compared to NRMSE(γ). For model $\mathcal{B}_4$, it is the other way around.

6.5.2. *Model group $\mathcal{D}$* In terms of NRMSE(γ) (25) and RMSE(p) (26) model group $\mathcal{D}$ behaves as expected, and obeys the rule: the higher the complexity is, the higher the accuracy becomes. According to the RMSE(p) column in table 7, the models in $\mathcal{D}$ all introduce an RMSE(p) which is less than that found for the measurement noise. Comparing models $\mathcal{D}_1$ (21) and $\mathcal{D}_2$ (22), it is obvious that not much is gained in accuracy by using the unburned specific heats from CHEPP instead of the linear functions. The computational cost for $\mathcal{D}_2$ was more than two times the one for $\mathcal{D}_1$, as shown in table 5. This suggests that the unburned specific heats are sufficiently well described by the linear approximation. Model $\mathcal{D}_3$ (23) utilizes the burned specific heat

from CHEPP, and this is an improvement compared to model $\mathcal{D}_1$ which uses the Krieger-Borman polynomial for $c_{p,b}$ and $c_{v,b}$. This improvement reduces the RMSE(p) with a factor 7, but the cost in computational time is high, approximately a factor 70 according to table 5. This is considered to be a too high cost at the moment. The comparison also shows that if we want to reduce the impact on the cylinder pressure, the effort should be to increase the accuracy of the Krieger-Borman polynomial for the burned mixture. This is however left as future work for the moment, and in the meanwhile model $\mathcal{D}_1$ is recommended as a good compromise between computational accuracy and efficiency.

6.5.3. *Model group $\mathcal{C}$* In model group $\mathcal{C}$, model $\mathcal{C}_5$ has good performance when considering the NRMSE in γ (25), but not as good in RMSE(p) (26). This perhaps explains why Chun and Heywood (1987) consider this to be a good and accurate enough model for single-zone models. This illustrates the importance of evaluating the modeling error in the γ-domain to the cylinder pressure domain, and it also reflects that RMSE(p) is the more important model performance measure of the two. Model $\mathcal{C}_2$ (Stone, 1999, p.423) has really bad performance and would be the last choice here. The rest of the models in group $\mathcal{C}$ obeys the same rule as group $\mathcal{D}$, i.e. $\mathcal{C}_4 \prec \mathcal{C}_3 \prec \mathcal{C}_1$.

When the best model in group $\mathcal{C}$, i.e. $\mathcal{C}_4$, is compared to all models in group $\mathcal{D}$, and especially the reference model $\mathcal{D}_4$, it is concluded that the specific heats should be interpolated, and not the specific heat ratios. This conclusion can be drawn since the only difference between $\mathcal{C}_4$ and $\mathcal{D}_4$ is how the interpolation is performed. Model $\mathcal{C}_4$ interpolates the specific heat ratios found from CHEPP directly, and model $\mathcal{D}_4$ interpolates the specific heats from CHEPP and then form the specific heat ratio. Therefore, group $\mathcal{D}$ has better performance than group $\mathcal{C}$. Since $\mathcal{D}_1$ has higher accuracy and approximately the same computational time as all models in group $\mathcal{C}$, there is no point in using any of the models in group $\mathcal{C}$.

6.5.4. *Model group $\mathcal{B}$* As expected, the models in group $\mathcal{B}$ has the worst performance of them all, if excluding models $\mathcal{C}_2$ and $\mathcal{C}_5$. It is interesting to note that the linear model γ_{lin}^b ($\mathcal{B}_1$) performs best in the group, although it introduces a modeling error in p which is at least ten times the measurement noise in the mean. It has better performance than γ_{KB} ($\mathcal{B}_3$) in the pressure domain, although this is not the case in the γ-domain. This again points out the necessity of evaluating the impact of the γ-model on to the cylinder pressure. Therefore, if the assumption is that the cylinder contents should be treated as a burned mixture during the entire closed part of the engine cycle, $\mathcal{B}_1$ is the model to use.

6.5.5. *Summary* To conclude, the models are ordered by their performance and with computational efficiency in ascending order:

$$\mathcal{D}_4 \prec \mathcal{D}_1 \prec \mathcal{B}_1 \prec \mathcal{B}_4 \qquad (27)$$

Some of the models are excluded from this list, either due to their low accuracy, high computational time, or because another model with approximately the same computational time has higher accuracy. Of the models given in (27), $\mathcal{D}_1$ is recommended as a compromise between computational time and accuracy. Compared to the original setting in Gatowski et al. (1984), the computational burden increases with 40 % and the modeling error is more than ten times smaller in the mean. This also stresses that the γ-model is an important part of the heat release model, since it has a large impact on the cylinder pressure. The focus is now turned to how the γ-models will affect the heat release parameters.

6.6 Influence of γ-models on heat release parameters

The question is: What impact does each of the proposed γ-models have on the heat release parameters? This is investigated by using the cylinder pressure for operating point 2, given in figure 7, and estimate the three heat release parameters θ_d, θ_b and Q_{in} in the Vibe function, introduced in appendix C. The cylinder pressure is simulated using reference model $\mathcal{D}_2$ in conjunction with the Gatowski et al. cylinder pressure model, and this forms the cylinder pressure measurement signal to which measurement noise is added.

The heat release trace is then estimated given the measurement from reference model $\mathcal{D}_2$. The heat release trace is parameterized by the Vibe function, which has the heat release parameters θ_d, θ_b and Q_{in}. The estimation is performed by minimizing the prediction error, i.e. by minimizing the difference between the measured cylinder pressure and the modeled cylinder pressure. The Levenberg-Marquardt method is used as optimization algorithm. The heat release parameters are then estimated for each of the γ-models using the Gatowski et al.-model, where the γ-model is replaced in an obvious manner in the equations. In the estimations, only the three heat release parameters are estimated. The other parameters are set to their true values given in table E.1. The results are summarized in table 8, which displays the relative estimation error (RE) and the relative 95 % confidence interval (RCI) in θ_d, θ_b and Q_{in} respectively for each γ-model. The computational time and RMSE(p) are also given.

6.6.1. *Discussion* The RMSE of the applied measurement noise is approximately 6.7 kPa, which is also the RMSE found when using most γ-models. All methods are able to estimate the rapid burn angle θ_b most accurately of the three, and almost all of them are accurate within 1%. On the other hand, only model group $\mathcal{D}$ is accurate within 1 %

	θ_d [%]		θ_b [%]		Q_{in} [%]		RMSE [kPa]
	RE	RCI	RE	RCI	RE	RCI	
$\mathcal{B}_1$	5.1	1.7	0.29	3.1	-9.2	1.4	9.8
$\mathcal{B}_2$	3.1	1.7	0.63	2.9	-7.3	1.3	9.1
$\mathcal{B}_3$	3.4	1.7	-0.2	2.9	-7.2	1.3	9.1
$\mathcal{B}_4$	6.8	1.7	-0.11	3.2	-6.2	1.4	10.1
$\mathcal{C}_1$	0.074	1.4	1.1	2.4	-2.9	1.1	6.5
$\mathcal{C}_2$	9.6	2.1	-1	3.9	-14	1.7	16.0
$\mathcal{C}_3$	0.19	1.4	0.75	2.4	-2.5	1.2	6.5
$\mathcal{C}_4$	0.14	1.5	0.64	2.4	-2	1.2	6.7
$\mathcal{C}_5$	-8	1.5	-2.5	2.3	27	0.92	6.6
$\mathcal{D}_1$	0.21	1.5	-0.062	2.4	-0.67	1.3	6.7
$\mathcal{D}_2$	0.2	1.5	-0.08	2.4	-0.61	1.3	6.7
$\mathcal{D}_3$	0.22	1.5	-0.13	2.4	-0.48	1.3	6.7
$\mathcal{D}_4$	0.21	1.5	-0.13	2.4	-0.42	1.3	6.7

Table 8. Relative estimation error (RE) and relative 95 % confidence interval (RCI) given in per cent, for heat release parameters using various γ-models at operating point 2. The nominal values for the heat release parameters are: $\theta_d = 15$ deg, $\theta_b = 30$ deg and $Q_{in} = 760$ J. The computational time and cylinder pressure RMSE are also given.

for all three parameters, and this suggests that any of the $\mathcal{D}$-models can be used, preferably model $\mathcal{D}_1$ due to its lower computational time. Note also that $\mathcal{C}_5$ gives the highest deviation in the estimates of them all.

6.7 Influence of air-fuel ratio λ

An investigation is performed to see how the proposed model $\mathcal{D}_1$ behaves for different air-fuel ratios λ. The NRMSE($\gamma;\mathcal{D}_1,\lambda$) and RMSE($p;\mathcal{D}_1,\lambda$) are computed for model $\mathcal{D}_1$ (21) compared to reference model $\mathcal{D}_4$ for air-fuel ratio $\lambda \in [0.975, 1.025]$, at operating point 2. It is assumed that the λ-controller of the SI engine has good performance, and therefore keeps the variations in λ small. The results are displayed in figure 11, where the upper plot shows the NRMSE($\gamma;\mathcal{D}_1,\lambda$), and the lower plot shows the RMSE($p;\mathcal{D}_1,\lambda$). Lean and stoichiometric mixtures have the lowest errors in the γ domain, which is
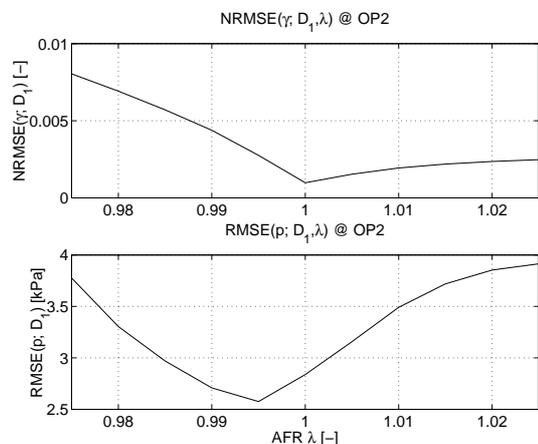

Fig. 11. *Upper:* NRMSE($\gamma;\mathcal{D}_1,\lambda$) for $\lambda \in [0.975, 1.025]$. *Lower:* RMSE($p;\mathcal{D}_1,\lambda$) for $\lambda \in [0.975, 1.025]$.

expected since the Krieger-Borman polynomial for the burned mixture is estimated for lean mixtures. The error in pressure domain is approximately symmetric around $\lambda = 0.995$, and the magnitude is still less than the measurement noise. This assures that for a few per cent deviation in λ from stoichiometric conditions, the introduced error is still small and acceptable.

6.7.1. *A note on fuel composition*   An sensitivity analysis is made for fuels such as methane and two commercial fuels in (Klein, 2004). This in order to see if the results are valid for other fuels than iso-octane. The carbonhydrogen ratio for the fuel $C_a H_b$ is given by $y = b/a$. It is found that the hydrocarbon ratio needs to be close to 2.25, i.e. the one for iso-octane, although an exact limit can not be given without further studies. For a commercial fuel with ratio $y = 1.88$, the RMSE(p) introduced is increased with less than 75 % compared to iso-octane, which is acceptable.

6.8 *Influence of residual gas*

The influence of the residual gas mass fraction x_r on the specific heat ratio has been investigated in (Klein, 2004). It was found that the model used needs to be robust to changing operating conditions, a feature the Krieger-Borman polynomial has. Therefore model (28) which uses the Krieger-Borman polynomial is recommended, although it did not have the best performance of the x_r-models at every operating point.

$$c_p = x_b c_{p,b}^{KB}(T_b, p) + (1 - x_b) \left((1 - x_r)c_{p,u}^{lin}(T_u) + x_r c_{p,b}^{KB}(T_u, p) \right) \tag{28a}$$

$$c_v = x_b c_{v,b}^{KB}(T_b, p) + (1 - x_b) \left((1 - x_r)c_{v,u}^{lin}(T_u) + x_r c_{v,b}^{KB}(T_u, p) \right) \tag{28b}$$

$$\gamma_{\mathcal{D}_{1x_r}}(T, p, x_b, x_r) = \frac{c_p(T, p, x_b, x_r)}{c_v(T, p, x_b, x_r)} \tag{28c}$$

6.9 *Summary for partially burned mixture*

The results can be summarized as:

- The modeling error must be compared both in terms of how they describe γ and the cylinder pressure.
- Comparing models $\mathcal{C}_4$ and $\mathcal{D}_4$, it is obvious that interpolating the specific heat ratios directly instead of the specific heats causes a large pressure error. Interpolation of specific heat ratios does not fulfill the energy equation.
- The γ-models $\mathcal{B}_1$, $\mathcal{B}_2$, $\mathcal{B}_3$, $\mathcal{B}_4$, $\mathcal{C}_2$ and $\mathcal{C}_5$ proposed in earlier works, introduce a pressure modeling error which is at least four times the measurement noise, and at least ten times the measurement noise in the mean. If any of them should be used, model $\mathcal{B}_1$ should be considered.
- If only single-zone temperatures are allowed, model $\mathcal{B}_1$ is the better one.

- The computation times are of the same order for all models except $\mathcal{D}_3$, $\mathcal{D}_4$ and $\mathcal{C}_4$.
- The models in group $\mathcal{D}$ are required to get a cylinder pressure RMSE that is of the same order as the measurement noise.
- As a compromise between accuracy and computational time, model $\mathcal{D}_1$ is recommended. Compared to the original setting in Gatowski et al. (1984), the computational burden increases with 40 % and the cylinder pressure modeling error is 15 times smaller in mean.
- For a residual gas mass fraction x_r up to 20 %, model $\mathcal{D}_1$ can be extended with specific heats for the residual gas (28). These specific heats are modeled by the Krieger-Borman polynomial. This model extension adds a NRMSE(γ) which is less than 0.3 % to the previous modeling error for $x_r = 0$.
- The results are valid for the air-fuel ratio region $\lambda \in [0.975, 1.025]$ with retained accuracy. For other fuels than iso-octane, the hydrogen-carbon ratio y needs to be close to 2.25, i.e. the one for iso-octane. The closer, the better the accuracy is. For a commercial fuel with ratio $y = 1.88$, the RMSE(p) is increased with 70 % compared to iso-octane for model $\mathcal{D}_1$, which is acceptable.
- Only model group $\mathcal{D}$ produces prediction error estimates of the heat release parameters, that are accurate within 1 % for all three parameters, and this suggests that any of the $\mathcal{D}$-models can be used, preferably model $\mathcal{D}_1$ due to its lower computational time.

7. CONCLUSIONS

Based on assumptions of frozen mixture for the unburned mixture and chemical equilibrium for the burned mixture, the specific heat ratio is calculated, using a full equilibrium program (Eriksson, 2004), for an unburned and a burned air-fuel mixture, and compared to several previously proposed models of γ. It is shown that the specific heat ratio and the specific heats for the unburned mixture is captured within 0.25 % by a linear function in mean charge temperature T for $\lambda \in [0.8, 1.2]$, and the burned mixture is captured within 1 % by a higher-order polynomial in cylinder pressure p and temperature T developed in Krieger and Borman (1967) for the major operating range of a spark ignited (SI) engine. If a linear model is prefered for computational reasons for the burned mixture, the temperature region should be chosen with care which can reduce the modeling error in γ by 25 %.

With the knowledge of how to describe γ for the unburned and burned mixture respectively, the focus is turned to finding a γ-model during the combustion process, i.e. for a partially burned mixture. This is done by interpolating the specific heats for the unburned and burned mixture using the mass fraction burned x_b. The objective of the work was to find a model of γ, which results in a cylinder

pressure error less than or in the order of the measurement noise. It is found that interpolating the linear specific heats for the unburned mixture and the higher-order polynomial specific heats for the burned mixture, and then forming the specific heat ratio

$$\gamma(T, p, x_b) = \frac{c_p(T, p, x_b)}{c_v(T, p, x_b)} = \frac{x_b\, c_{p,b}^{KB} + (1 - x_b)\, c_{p,u}^{lin}}{x_b\, c_{v,b}^{KB} + (1 - x_b)\, c_{v,u}^{lin}}$$
(29)

results in a small enough modeling error in γ. This modeling error results in a cylinder pressure error less than 6 kPa in mean, which is in the same order as the cylinder pressure measurement noise.

It was also shown that it is important to evaluate the model error in γ to see what impact it has on the cylinder pressure, since a small error in γ can yield a large cylinder pressure error. This also stresses that the γ-model is an important part of the heat release model.

Applying the proposed model improvement, model $\mathcal{D}_1$ (29), of the specific heat ratio to the Gatowski et al. (1984) single-zone heat release model is simple, and it only increases the computational burden slightly. Compared to the original model, the computational burden increases with 40 % and the modeling error introduced in the cylinder pressure is reduced by a factor 15 in mean.

References

I. Andersson. Cylinder pressure and ionization current modeling for spark ignited engines. Technical report, Vehicular Systems, 2002. LiU-TEK-LIC-2002:35, Thesis No. 962.

M.F.J. Brunt, A. Rai, and A.L. Emtage. The calculation of heat release energy from engine cylinder pressure data. In *SI Engine Combustion*, 1998. SAE Technical Paper 981052.

K. M. Chun and J. B. Heywood. Estimating heat-release and mass-of-mixture burned from spark-ignition engine pressure data. *Combustion Sci. and Tech.*, Vol. 54:133–143, 1987.

L. Eriksson. Requirements for and a systematic method for identifying heat-release model parameters. *Modeling of SI and Diesel Engines*, SP-1330:19–30, 1998. SAE Technical Paper no.980626.

L. Eriksson. *Spark Advance Modeling and Control*. PhD thesis, Linköping University, May 1999. ISBN 91-7219-479-0, ISSN 0345-7524.

L. Eriksson. Chepp –a chemical equilibrium program package for matlab. volume SP-1830, 2004. SAE Technical Paper 2004-01-1460.

J.A. Gatowski, E.N. Balles, K.M. Chun, F.E. Nelson, J.A. Ekchian, and J.B. Heywood. Heat release analysis of engine pressure data. 1984. SAE Technical Paper 841359.

Y.G. Guezennec and W. Hamama. Two-zone heat release analysis of combustion data and calibration of heat transfer correlation in an I.C. engine. 1999. SAE Technical paper 1999-01-0218.

J. B. Heywood. *Internal Combustion Engine Fundamentals*. McGraw-Hill series in mechanical engineering. McGraw-Hill, 1988. ISBN 0-07-100499-8.

M. Klein. A specific heat ratio model and compression ratio estimation. Licentiate thesis, Vehicular Systems, Linköping University, 2004. LiU-TEK-LIC-2004:33, Thesis No. 1104.

M. Klein and L. Eriksson. A specific heat ratio model for single-zone heat release models. *Modeling of SI Engines*, SP-1830, 2004. SAE Technical Paper 2004-01-1464.

R.B. Krieger and G.L. Borman. The computation of apparent heat release for internal combustion engines. *ASME*, 1967.

F.A. Matekunas. Modes and measures of cyclic combustion variability. 1983. SAE Technical Paper 830337.

Y. Nilsson and L. Eriksson. A new formulation of multi-zone combustion engine models. IFAC Workshop: Advances in Automotive Control, pages 629–634, Karlsruhe, Germany, 2001.

R. Stone. *Introduction to Internal Combustion Engines*. SAE International, 3rd edition, 1999.

R.A. Svehla and B.J. McBride. Fortran iv computer programs for calculation of thermodynamic and transport properties of complex chemical systems. Technical Report NASA Technical Note TND-7056, NASA Lewis Research Center, 1973.

I.I. Vibe. *Brennverlauf und Kreisprocess von Verbennungsmotoren*. VEB Verlag Technik Berlin, 1970. German translation of the russian original.

Appendix A. TEMPERATURE MODELS

Two models for the in-cylinder temperature will be described, the first is the mean charge single-zone temperature model. The second is a two-zone mean temperature model, used to compute the single-zone thermodynamic properties as mean values of the properties in a two-zone model.

A.1 *Single-zone temperature model*

The mean charge temperature T for the single-zone model is found from the state equation $pV = m_c R T$, assuming the total mass of charge m_c and the mass specific gas constant R to be constant. These assumptions are reasonable since the molecular weights of the reactants and the products are essentially the same (Gatowski et al., 1984). If all thermodynamic states $(p_{ref}, T_{ref}, V_{ref})$ are known/evaluated at a given reference condition ref, such as IVC, the mean charge temperature T is computed as

$$T = \frac{T_{IVC}}{p_{IVC} V_{IVC}} pV \qquad \text{(A.1)}$$

A.2 Two-zone mean temperature model

A two-zone model is divided into two zones; one containing the unburned gases and the other containing the burned gases, separated by a infinitesimal thin divider representing the flame front. Each zone is homogeneous considering temperature and thermodynamic properties, and the pressure is the same throughout all zones (Nilsson and Eriksson, 2001). Here a simple two-zone model will be used to find the burned zone temperature T_b and the unburned zone temperature T_u, in order to find a more accurate value of $\gamma(T)$ as an interpolation of $\gamma_u(T_u)$ and $\gamma_b(T_b)$. The model is called temperature mean value approach (Andersson, 2002), and is based on a single-zone combustion model and adiabatic compression of the unburned charge. The single-zone temperature can be seen as a mass-weighted mean value of the two zone temperatures.

Prior to start of combustion (SOC), the unburned zone temperature T_u equals the single-zone temperature T:

$$T_{u,SOC} = T_{SOC} \qquad (A.2)$$

The unburned zone temperature T_u after SOC is then computed assuming adiabatic compression of the unburned charge according to:

$$T_u = T_{u,SOC}\left(\frac{p}{p_{SOC}}\right)^{1-1/\gamma} = T_{SOC}\left(\frac{p}{p_{SOC}}\right)^{1-1/\gamma} \qquad (A.3)$$

The unburned zone temperature T_u is therefore given by:

$$T_u(\theta) = \begin{cases} T(\theta) & \theta \le \theta_{ig} \\ T(\theta_{ig})\left(\frac{p}{p(\theta_{ig})}\right)^{1-1/\gamma} & \theta > \theta_{ig} \end{cases} \qquad (A.4)$$

Energy balance between the single-zone and the two-zone models yields:

$$(m_b + m_u)c_v T = m_b c_{v,b} T_b + m_u c_{v,u} T_u \qquad (A.5)$$

Assuming $c_v = c_{v,b} = c_{v,u}$, i.e. a calorically perfect gas, ends up in

$$T = \frac{m_b T_b + m_u T_u}{m_b + m_u} = x_b T_b + (1 - x_b)T_u \qquad (A.6)$$

where the single-zone temperature can be seen as the mass-weighted mean temperature of the two zones. Including a model for c_v would increase the importance of T_b in (A.6), resulting in a lower value for T_b. From (A.6), T_b is found as

$$T_b = \frac{T - (1 - x_b)T_u}{x_b} \qquad (A.7)$$

The procedure is summarized as:

(1) Compute the single-zone temperature T in (A.1)

(2) Compute the mass fraction burned x_b by using e.g. Matekunas pressure ratio management (C.1) and use the Vibe function in (C.3) to parameterize the solution

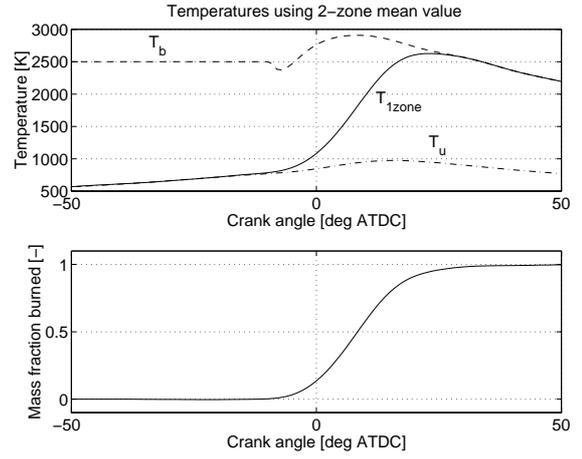(3) Compute the unburned zone temperature T_u using (A.4)

Fig. A.1. *Upper:* Single-zone temperature T_{1z}, unburned T_u and burned T_b zone temperatures for the cylinder pressure given in figure 7. *Bottom:* Corresponding mass fraction burned trace calculated using Matekunas pressure ratio.

(4) Compute the burned zone temperature T_b from (A.7)

The various zone temperatures for the cylinder pressure trace displayed in figure 7 are shown in figure A.1. The burned zone temperature is sensitive to low values of the mass fraction burned, x_b. Therefore, T_b is set to the adiabatic flame temperature for $x_b < 0.01$. The adiabatic flame temperature T_{ad} for a constant pressure process is found from:

$$h_u(T_u) = h_b(T_{ad}, p) \qquad (A.8)$$

where h_u and h_b are the enthalpy for the unburned and burned mixture respectively.

Appendix B. CYLINDER PRESSURE MODEL

The article (Gatowski et al., 1984) develops, tests and applies the cylinder pressure model used here. It maintains simplicity while still including the effects of heat transfer and crevice flows. The model has been widely used and the phenomena that it takes into account are well known (Heywood, 1988). The pressure differential dp can be written as

$$dp = \frac{\text{đ}Q_{ch} - \frac{\gamma}{\gamma-1}\,p\,dV \,-\, \text{đ}Q_{ht}}{\frac{1}{\gamma-1}\,V \,+\, \frac{V_{cr}}{T_w}\left(\frac{T}{\gamma-1} - \frac{1}{b}\ln\left(\frac{\gamma-1}{\gamma'-1}\right) + T'\right)} \qquad (B.1)$$

This is an ordinary differential equation that easily can be solved numerically if a heat-release trace $\text{đ}Q_{ch}$ is provided. The heat release is modeled by the Vibe function described in section C.

Appendix C. COMBUSTION MODEL

The combustion of fuel and air is a very complex process, and would require extensive modeling to fully capture. Our approach here is to use the pressure ratio management (Matekunas, 1983) to

produce a mass fraction burned trace and then use the Vibe function to parameterize the burn rate of the combusted charge. If the mass fraction burned trace is known, as for simulations, the pressure ratio management is not used.

C.1 *Matekunas pressure ratio*

The pressure ratio management was developed by Matekunas (1983) and is defined as the ratio of the cylinder pressure from a firing cycle $p(\theta)$ and the corresponding motored cylinder pressure $p_m(\theta)$:

$$PR(\theta) = \frac{p(\theta)}{p_m(\theta)} - 1 \qquad (C.1)$$

The mass fraction burned trace x_b is then approximated by the normalized pressure ratio $PR_N(\theta)$

$$x_b(\theta) \approx PR_N(\theta) = \frac{PR(\theta)}{\mathbf{max}PR(\theta)} \qquad (C.2)$$

an approximation valid within 1-2 degrees (Eriksson, 1999).

C.2 *Vibe function*

The Vibe function (Vibe, 1970) is often used as a parameterization of the mass fraction burned x_b, and it has the following form

$$x_b(\theta) = 1 - e^{-a\left(\frac{\theta - \theta_{ig}}{\Delta\theta}\right)^{m+1}} \qquad (C.3)$$

The burn rate is given by its differentiated form

$$\frac{dx_b(\theta)}{d\theta} = \frac{a\,(m+1)}{\Delta\theta}\left(\frac{\theta - \theta_{ig}}{\Delta\theta}\right)^m e^{-a\left(\frac{\theta - \theta_{ig}}{\Delta\theta}\right)^{m+1}} \qquad (C.4)$$

where θ_{ig} is the start of the combustion, $\Delta\theta$ is the total combustion duration, and a and m are adjustable parameters. In (Klein, 2004, p.32) the eqations to relate the parameters a and m to the physical burn angle parameters θ_d and θ_b are given.

The differentiated Vibe function (C.4) is used to produce a mass fraction burned trace, i.e. a normalized heat-release trace. The absolute value of the heat-release rate $\frac{dQ_{ch}}{d\theta}$ is given by the fuel mass m_f, the specific heating value of the fuel q_{HV}, and combustion efficiency η_f as

$$\frac{dQ_{ch}}{d\theta} = m_f q_{HV} \eta_f \frac{dx_b}{d\theta} = Q_{in}\frac{dx_b}{d\theta} \qquad (C.5)$$

where Q_{in} represents the total energy released from combustion.

Summing up, the combustion process is described by (C.5), parameterized by Q_{in}, θ_{ig}, θ_d, and θ_b.

Appendix D. ALTERED CREVICE TERM

The energy term describing the energy lost when a mass element enters the crevice volume depends on which γ-model is used and therefore has to be restated for every γ-model except $\mathcal{B}_1$, which was done in (B.1) for the original setting in the Gatowsk et.al. model. Details are found in (Klein, 2004). For model $\mathcal{D}_1$, the energy term $u' - u$ is therefore rewritten as:

$$u' - u = \int_T^{T'} c_v\, dT$$
$$= x_b \int_T^{T'} c_{v,b}^{KB}\, dT + (1 - x_b)\int_T^{T'} c_{v,u}^{lin}\, dT$$
$$= x_b(u^{KB}(T') - u^{KB}(T)) + (1 - x_b)\frac{R}{b^u}\ln\left(\frac{\gamma_{lin}^u(T') - 1}{\gamma_{lin}^u(T) - 1}\right) \tag{D.1}$$

where we have used that $c_v = x_b c_{v,b}^{KB} + (1 - x_b)c_{v,u}^{lin}$ in the second equality, and in the third equality that $c_v = (\frac{\partial u}{\partial T})_V$ for the burned mixture and (1) for the linear unburned mixture. The first term in (D.1) is given directly by the Krieger-Borman polynomial in it is original form. The second term is easily computed when knowing the coefficient values for the linear unburned mixture model, i.e.

$$\gamma_{lin}^u = \gamma_{300}^u + b^u(T - 300) \qquad (D.2)$$

Note that (D.1) is zero whenever $T' = T$, i.e. when the mass flow is out of the modeled crevice volume.

Appendix E. SINGLE ZONE MODEL PARAMETERS

Par.	Description	Value
γ_{300}	constant specific heat ratio [-]	1.3678
b	slope for specific heat ratio[K^{-1}]	$-8.13 \cdot 10^{-5}$
C_1	heat-transfer parameter [-]	2.28
C_2	heat-transfer parameter [-]	$3.24 \cdot 10^{-3}$
θ_0	crank angle phasing [deg ATDC]	0.4
Δp	bias in pressure measurements [kPa]	30
K_p	pressure measurement gain[-]	1
p_{ivc}	cylinder pressure at IVC [kPa]	100
T_{ivc}	mean charge temperature at IVC [K]	340
T_w	mean wall temperature [K]	440
V_c	clearance volume [cm^3]	35.5
V_{cr}	single aggregate crevice volume [% V_c]	1
θ_{ig}	ignition angle [deg ATDC]	-20
θ_d	flame-development angle [deg ATDC]	15
θ_b	rapid-burn angle [deg ATDC]	30
Q_{in}	released energy from combustion [J]	760

Table E.1. Nominal values for the parameters in the Gatowski et al. single-zone heat release model.